



## XANES AND EXAFS STRUCTURAL STUDIES OF BIOLOGICALLY RELEVANT COPPER (II) COMPLEXES OF ARYLHYDRAZONE DERIVATIVES

Pankaj Agrawal<sup>1\*</sup>, Pradeep Sharma<sup>2</sup>, Ashutosh Mishra<sup>3</sup>

### Abstract:

X-Ray absorption fine structure studies of Schiffbase copper(II) complexes were performed. Arylhydrazone derivatives, a primary ligand of copper complexes used in the study, were 5,5-dimethyl-(2-(4-nitrophenyl)hydrazono)cyclohexane-1,3-dione and 5,5-dimethyl-(2-(4-chlorophenyl)hydrazono) cyclohexane-1,3-dione. The crystalline nature and presence of specific functional groups of the copper (II) complexes were confirmed by X-ray diffraction (XRD) and Fourier Transform Infrared Spectroscopy (FTIR), respectively. The X-ray absorption near edge structure (XANES) data have been analyzed to calculate the K-edge shift, principal absorption maximum shift, edge width, and chemical shift. The experimental value of chemical shift is in accordance with the principal absorption maximum shift, indicating that the copper is in an oxidation state +2 in the sample. Effective nuclear charge (ENC) and percentage covalency were calculated from chemical shift and edge width, respectively. The first shell bond length was calculated using extended X-ray absorption fine structure (EXAFS) following different graphical methods. Fourier transforms of the normalized spectra have also been used to obtain bond length.

**Keywords:** XANES, EXAFS, XRD, FTIR, Chemical Shift, Athena, Edge Width

---

<sup>1\*</sup>Govt. Polytechnic College, Sendhwa, Madhya Pradesh, India Email: pankajphd02@gmail.com

<sup>2</sup>Govt. Holkar (Model, Autonomous) Science College, Indore, Madhya Pradesh, India

<sup>3</sup>School of Physics, Devi Ahilya University, Khandwa Road, Indore, Madhya Pradesh, India

**\*Correspondence Author:** Pankaj Agrawal

\*Govt. Polytechnic College, Sendhwa, Madhya Pradesh, India Email: pankajphd02@gmail.com

**DOI:** - 10.48047/ecb/2023.12.si5a.077

## 1. Introduction:

In many different domains, including analytical, biological, and inorganic chemistry, Schiff base copper(II) complexes are among the most frequently utilized classes of organic molecules. Due to a wide range of biological actions, including anti-inflammatory, analgesic, antibacterial, anti-convulsant, antitubercular, anticancer, antioxidant, and so forth, Schiff bases have grown in importance in the medical and pharmaceutical industries [1,2]. As building blocks for prospective anti-diabetic medications, aryl hydrazones of cyclic 1-3 diones have been widely employed [3-6]. Additionally, these complexes were employed as medications for cardiovascular disease, cancer, and anti-inflammation [7-11]. In particular chemical reactions, such as the Henny reaction, it functions as an active catalyst [12]. Copper (II) complexes are also the essential components of supramolecular devices because of their advantageous excited state and quantifiable characteristics. The use of copper complexes is also advantageous in photochemistry, photophysics, and biochemistry. Because of their utility, there is an expanding market for Schiff-base coordination complexes produced by reacting transition metal ions, especially copper. In the present paper, we investigated X-ray absorption fine structure XANES and EXAFS, X-ray diffraction XRD, and FTIR patterns of Cu (II) complexes of 5,5-dimethyl-2-(4-nitrohydrono) cyclohexane-1,3-dione (CL<sup>1</sup>) and 5,5-dimethyl-2-(4-chlorohydrono) cyclohexane-1,3-dione (CL<sup>2</sup>). X-ray absorption spectroscopy is an excellent tool to determine the electronic and geometrical structure of transition metal complexes. It helps in studying the structure around selected elements contained within a material at the atomic and molecular scales.

It can be applied to materials as well as crystals. This technique is classified into XANES (X-ray absorption near edge spectra) and EXAFS (Extended x-ray absorption fine structure). This study aims to determine the shift of K-edge, a shift of principal absorption maximum, edge width, chemical shift, effective nuclear charge (ENC), and percentage covalency from the XANES study. By EXAFS study, first shell bond lengths of complexes by three graphical methods, viz. Levy's, Lytle's, and LSS were determined. Fourier transforms of the normalized EXAFS spectra were used to calculate bond length. The XRD pattern was investigated to find crystalline structure, space group particle size, etc., and the FTIR pattern was used to confirm functional

groups present in the complexes. The purpose of determining the different parameters by XANES and EXAFS is to provide a better platform to study further biological, chemical, pharmaceutical, and medicinal properties that will help to predict the chemical behavior of complexes.

## 2. Experimental:

The samples were prepared by the method reported in the literature [13]. All the chemicals used are in pure grade. The Cu (II) complexes of 5,5-dimethyl-2-(4-nitrohydrono) cyclohexane-1,3-dione (CL<sup>1</sup>) and 5,5-dimethyl-2-(4-chlorohydrono) cyclohexane-1,3-dione (CL<sup>2</sup>) studied in this paper, has been synthesized by chemical route method at School of Chemistry, DAVV, Indore, India [13,14,15,16]. The chemicals used in the present work are 5,5-dimethylcyclohexane-1,3-dione (dimedone), 4-nitrophenyl, 4-chlorophenyl, ethanol, sodium hydroxide, sodium acetate, sodium nitrate, hydrochloric acid, Calcium chloride, Cu(Oac)<sub>2</sub>.2H<sub>2</sub>O. All the complexes synthesized are in powder form.

X-ray diffraction (XRD) is a resourceful non-destructive technique that gives perfect information about the chemical composition and crystallographic structure of materials [17]. The pattern has been indexed using joint committee for powder diffraction (JCPDF) software. The XRD pattern is made by using Bruker D-8, an advanced instrument at IUC, DAE-CSR, Indore, India. Complexes were characterized by XRD at room temperature and analyzed by the computer software OriginPro 2016.

Dispersive extended X-ray absorption fine structure (DEXAFS) beamline BL-8 at the 2.5 GeV synchrotron Indus-2 at RRCAT Indore, have been utilized for recording the X-ray absorption fine structure (XAFS) spectra according to the procedure outlined in ref. [18]. For the XAFS measurements appropriate amount of powder of complexes were thoroughly mixed with cellulose in a gate mortar and pressed in the form of a thin pellet. To select a band of energy from a white synchrotron beam, a bent crystal (Si 111) polychromator is used in this beamline, which is horizontally dispersed and focused on the sample. A position-sensitive CCD detector is used to record the transmitted beam intensity from the sample, thus the whole EXAFS spectrum around the absorption edge takes place in a single shot [18]. For data analysis computer program Athena (Demeter 0.9.25) was used available at the website xafs.org.

In the 4000-500 $\text{cm}^{-1}$ , the IR spectra were recorded at the School of Pharmacy, SGSITS Indore, India.

### 3. Result and discussion:

**3.1 X-Ray Diffraction:** The X-ray diffraction data of the 5,5- dimethyl-2-(4-nitrohydrazono) cyclohexane-1,3-dione ( $\text{CL}^1$ ) and 5,5- dimethyl-2-(4-chlorohydrazono) cyclohexane-1,3-dione( $\text{CL}^2$ ) were recorded at room temperature using Cu K $\alpha$  radiation. XRD patterns of the complexes were shown in figure 1 and figure 2. The pattern indicates poly crystalline nature of the complexes. The parameters calculated by the diffraction data were listed in Table-1. The diffraction pattern was recorded between  $2\theta$  ranging from  $0^\circ$  to  $60^\circ$ . The complexes were found in monoclinic crystal lattice with space group  $\text{P}1_21/n_1$  and  $\text{C}1_2/n_1$ . The

prominent peaks of the complexes have been identified by JCPDS software.

The average crystalline structure size was calculated by Debye Scherrer formula-

$$\sigma = \frac{K\lambda}{\beta \cos\theta}$$

Where  $K=0.9$  geometric factor  $\lambda=1.504\text{\AA}$  is the wavelength of X-rays,  $\theta$  is Bragg's angle,  $\beta$  is FWHM Full Width Half Maxima of main diffracted peaks [19] Dislocation density was calculated by the following relation-

$$\delta = \frac{1}{\sigma^2}$$

XRD pattern of complexes  $\text{CL}^1$  and  $\text{CL}^2$  are shown in following figure 1.

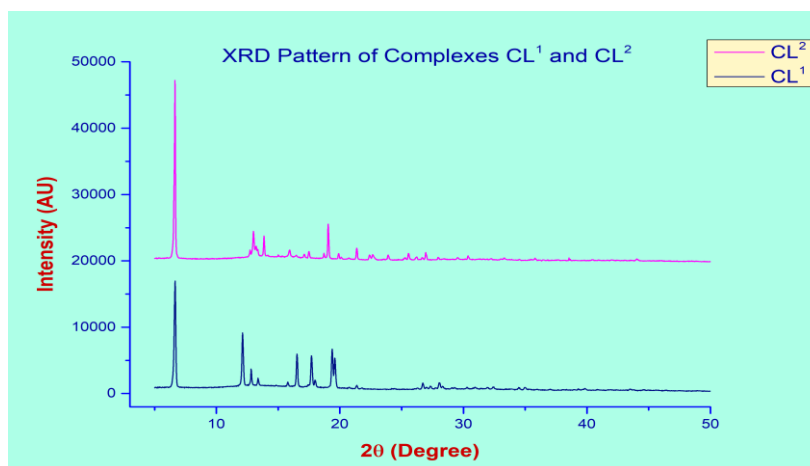


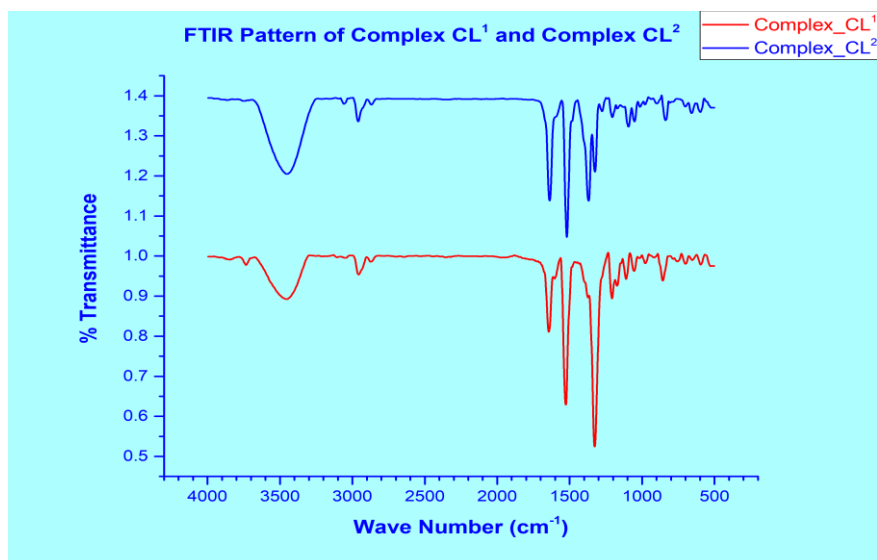
Figure 1. XRD Pattern of Complex  $\text{CL}^1$  and Complex  $\text{CL}^2$ .

Table-01- Crystallographic data for the complexes  $\text{CL}^1$  and  $\text{CL}^2$

	Complex- $\text{CL}^1$	Complex- $\text{CL}^2$
Empirical Formula	$\text{C}_{16}\text{H}_{19}\text{CuN}_3\text{O}_7$	$\text{C}_{16}\text{H}_{19}\text{CuClN}_2\text{O}_5$
Formula weight	428.88	418.33
Crystal System	Monoclinic	Monoclinic
Space group	$\text{P}1_21/n_1$	$\text{C}1_2/m_1$
a ( $\text{\AA}$ )	17.64	17.43
b ( $\text{\AA}$ )	14.63	20.20
c ( $\text{\AA}$ )	17.69	14.26
$\alpha^\circ$	90.00	90.00
$\beta^\circ$	104.46	106.52
$\gamma^\circ$	90.00	90.00
Volume ( $\text{\AA}^3$ )	4565.32	5020.75
Density( $\text{gram/cm}^3$ )	4.48	2.89
Particle size(nm)	36.67	37.95
Dislocation Density( $\text{nm}^{-2}$ )	$7.43 \times 10^{-4}$	$6.94 \times 10^{-4}$

**3.2 FTIR :** To identify functional groups (chemical bonds) present in compounds, FTIR is an effective investigation technique. In the 4000-500 $\text{cm}^{-1}$  region, the FTIR spectra of the  $\text{CL}^1$  and

$\text{CL}^2$  complexes were recorded. Figure 2 presents a comparison of the infrared spectra of the  $\text{CL}^1$  complex and the  $\text{CL}^2$  complex, measured in the 4000-500 $\text{cm}^{-1}$  region.



**Figure 2.** Combined FTIR Pattern of Ligand, Complex C1 and Complex C2.

Hydrated complexes are indicated by the presence of the water molecule indicated by  $\nu(\text{OH})$  group in the broad band of the region  $3445\text{--}3449\text{cm}^{-1}$  in the FTIR spectrum. The bands attributed to  $\nu(\text{C}=\text{O}$  and  $\text{C}=\text{O}\dots\text{H})$  observed in the FTIR at  $1674\text{ cm}^{-1}$  and  $1620\text{cm}^{-1}$ , respectively. The band in spectral region of  $2943\text{cm}^{-1}$  arises from a  $\nu(\text{NH})$  group. Strong bands corresponding to the range  $1387\text{--}1399\text{cm}^{-1}$  indicate the presence of a  $\nu(\text{COO}^-)$  coordinated carboxylate group. The peaks between  $3043$  and  $3086\text{ cm}^{-1}$  are depicted as  $(\text{CH}_{\text{arom}})$  stretching in the spectra of the complexes.

**3.3 XANES Study :** When a monochromatic beam of X-rays of energy  $E$ , passes through a homogeneous sample of the thickness  $x$ , then according to Lambert-Beer law –

$$\mu(E)x = \log\left(\frac{I_0}{I_t}\right)$$

Where  $I_0$  and  $I_t$  are the intensities of incident and transmitted X-rays,  $\mu(E)$  is the linear absorption coefficient, which describes how strongly X-rays are absorbed as a function of X-rays energy  $E$ . X-ray absorption fine structure are divided in two parts XANES and EXAFS region.[20-25].

XANES occurs in the region from the edge to approximately  $40\text{eV}$  above the edge. XANES are the result of multiple scattering [26]. First peak in the derivative spectrum indicates the position of first K-absorption edge  $E_k$ . The point where the derivative is zero, gives the position of principal absorption maxima (PAM)  $E_A$ .

The XAFS spectra have been plotted for Cu metal, Complexes  $\text{CL}^1$  and  $\text{CL}^2$  are shown in following figure 3. The curves in the figure 3 correspond to normalized K-absorption spectra.

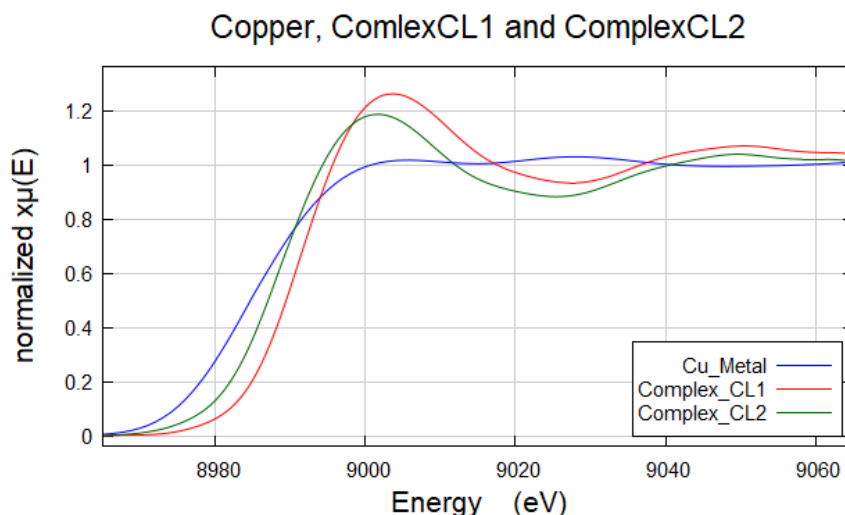


**Figure 3.** Normalized X-ray absorption spectra of Cu Metal, complexes  $\text{CL}^1$  and  $\text{CL}^2$ .

Derivative spectra shown in figure 4, the initial maxima specified the point of K-absorption edge

( $E_k$ ), and the initial minimum at zero derivatives match to the position of PAM ( $E_A$ ).

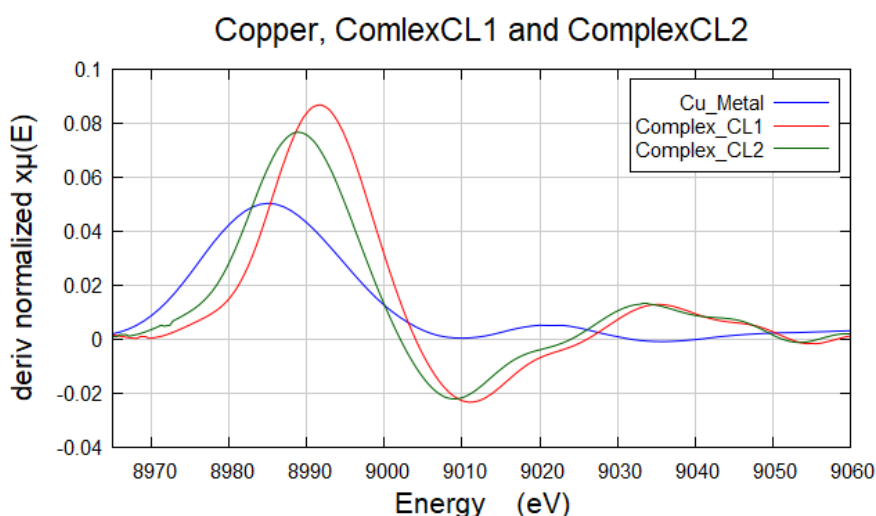


Figure 4. Derivate of XAFS spectra of Cu Metal, complexes CL<sup>1</sup> and CL<sup>2</sup>.

The summary of the calculated values of copper K-edge energies ( $E_k$ ), PAM ( $E_A$ ), chemical shift, edge width, ENC and percentage covalency of

Complexes CL<sup>1</sup> and CL<sup>2</sup> are given in following table 2.

Table 2. XANES data of Cu Metal, complexes CL<sup>1</sup> and CL<sup>2</sup>.

S No.	Metal / Complex	$E_k$ (eV)	$E_A$ (eV)	Chemical Shift (eV)	Shift of Principal Absorption Maxima PAM (eV)	Edge Width (eV)	ENC Electron /atom
1	Cu Metal	8985.03	9009.32	--	--	24.29	
2	Complex CL <sup>1</sup>	8991.58	9003.97	6.55	-5.35	12.39	0.45
3	Complex CL <sup>2</sup>	8988.78	9000.42	3.75	-8.9	11.64	0.26

**3.3.1. Chemical Shift:** The chemical shift is given as  $-\Delta E_k = E_k(\text{Complex}) - E_k(\text{Cu metal})$

Chemical shift data of the complex indicated that the copper metal has a +2 oxidation state in complexes. Chemical shifts of 6.55 eV and 3.75 eV were found for complexes CL<sup>1</sup> and CL<sup>2</sup>, respectively. Ionic bonding extends the chemical shift, while covalent bonding obstructed it [27].

**3.3.2. Principal Absorption Maxima (PAM):** The PAM is given as  $\Delta E_A = E_A(\text{Complex}) - E_A(\text{Cu metal})$

Table 2 shows that PAM moved to lower energies [27]. Moreover, the PAM shift of complex CL<sup>2</sup> was greater than that of complex CL<sup>1</sup>. As noted in Table 2, PAM shifted by -5.35 eV for complex CL<sup>1</sup> and -8.9 eV for complex CL<sup>2</sup>. The shift of PAM of complexes is in the opposite direction of chemical shifts. These reversible orders demonstrate that the change in the PAM is contrary correlated with the ionic nature of the

complexes. It can be concluded that copper is in the +2 oxidation state in this complex.

**3.3.3. Edge width:** In Table 2, edge width ( $E_A - E_k$ ) values were evaluated as 24.29 eV, 12.39 eV and 11.64 eV for Cu metal, complex CL<sup>1</sup> and complex CL<sup>2</sup>, respectively.

**3.3.4. Effective Nuclear Charge (ENC):** The ENC of copper in the complexes studied here is calculated to be 0.45 electrons/atom for complex CL<sup>1</sup> and 0.26 electrons/atom for complex CL<sup>2</sup> [28].

**3.4 EXAFS Study :** Beyond the edge by about 40 eV to 1000 eV, the EXAFS region increases [29]. In the current study, nearest neighbor bond lengths were calculated using Fourier transform methods and Levy's, Lytles, and L.S.S. used to compare results.

**3.4.1. Levy's Method:** By the Levy's Method, the bond length is given by-

$$R_1 = \left[ \frac{151}{\Delta E} \right]^{1/2}$$

Where  $\Delta E$  is the energy difference between the maximum B and minimum  $\beta$  in the EXAFS spectrum and  $R_1$  is the radius of the initial coordination sphere. Using the data calculated in Table3, bond lengths of 1.74Å and 1.72Å were determined for the complex CL<sup>1</sup> and complex CL<sup>2</sup>, respectively, as reported inTable4.[30].

**3.4.2. Lytle’s Method :** In Lytle’s Method the bond length is given by-

$$R_s = \left[ \frac{37.60}{M} \right]^{1/2}$$

Where M is the gradient of Q-E graph. Using the data calculated in Table3, bond lengths of 1.92Å and 1.90Å were determined for the complex CL<sup>1</sup>

and complex CL<sup>2</sup>, respectively, as reported in Table4. [31].

**3.4.3. L.S.S. Method :** The nearest neighbor distance ( $R_1 - \alpha_1$ ) is given by-

$$\frac{2(R_1 - \alpha_1)}{\pi} = \text{Slope of } k - n \text{ plot}$$

Using the data calculated in Table3, bond lengths of 1.21Å and 1.38Å were determined for the complex CL<sup>1</sup> and complex CL<sup>2</sup>, respectively, as reported inTable4.

**3.4.4. Fourier transform method :** Figure 7 shows the Fourier transform spectra obtained from the  $\chi(k)$ -k curves of complex CL<sup>1</sup> and complex CL<sup>2</sup>. The positions of the first peaks in the Fourier transform spectra provide the phase-corrected bond lengths (R) each for the complexCL<sup>1</sup> andcomplexCL<sup>2</sup>, as specified in Table 4. are, 1.35 Å, 1.49Å.

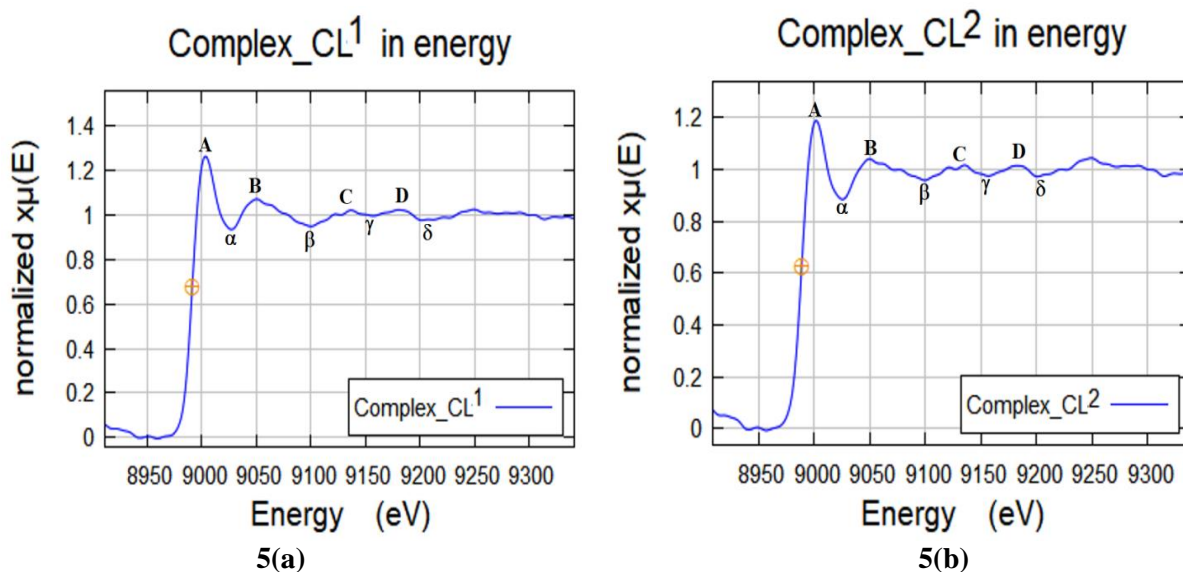


**Figure 5(a and b).**Normalized X-Ray absorption curves of complexes CL<sup>1</sup> and CL<sup>2</sup>.

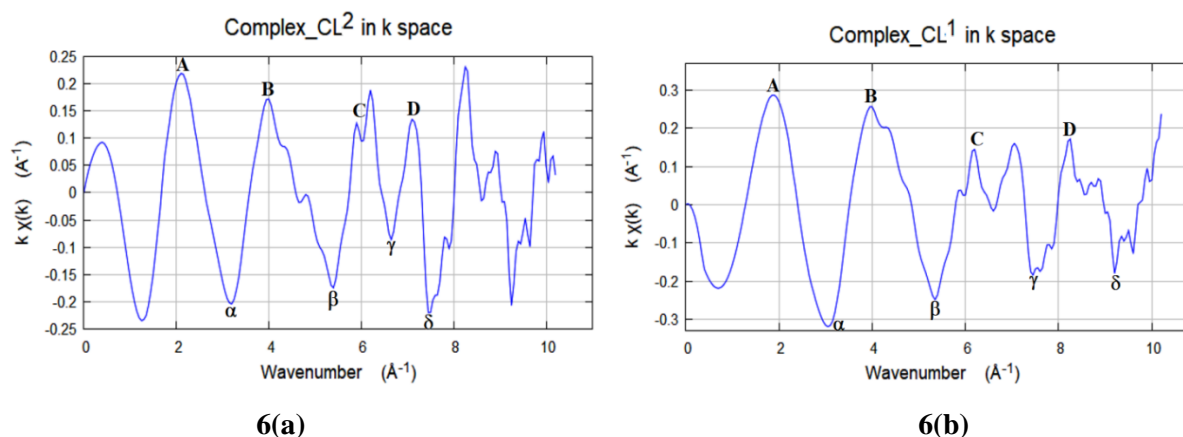


**Figure 6 (a and b).** $\chi(k)$ -k data of complexes CL<sup>1</sup> and CL<sup>2</sup>.

**Table 3.** Energy E(eV), wave vector k(Å<sup>-1</sup>) of complexes CL<sup>1</sup> and CL<sup>2</sup> obtained from Figures 5 and 6, the corresponding n values as well as energy level Q.

Structure	n	Q	Complex CL <sup>1</sup>		Complex CL <sup>2</sup>	
			E (eV)	k(Å <sup>-1</sup> )	E (eV)	k(Å <sup>-1</sup> )
A	0	2.04	11.88	1.90	12.90	2.10
α	1		36.31	3.07	36.39	3.19
B	2	6.04	58.30	4.07	60.94	4.01
α	3		107.98	5.35	111.44	5.40
C	4	12.00	136.49	6.59	137.68	610.11
α	5		167.44	7.65	167.91	6.66
D	6	20.00	192.24	8.23	196.54	7.11
α	7		209.81	9.20	210.06	7.52

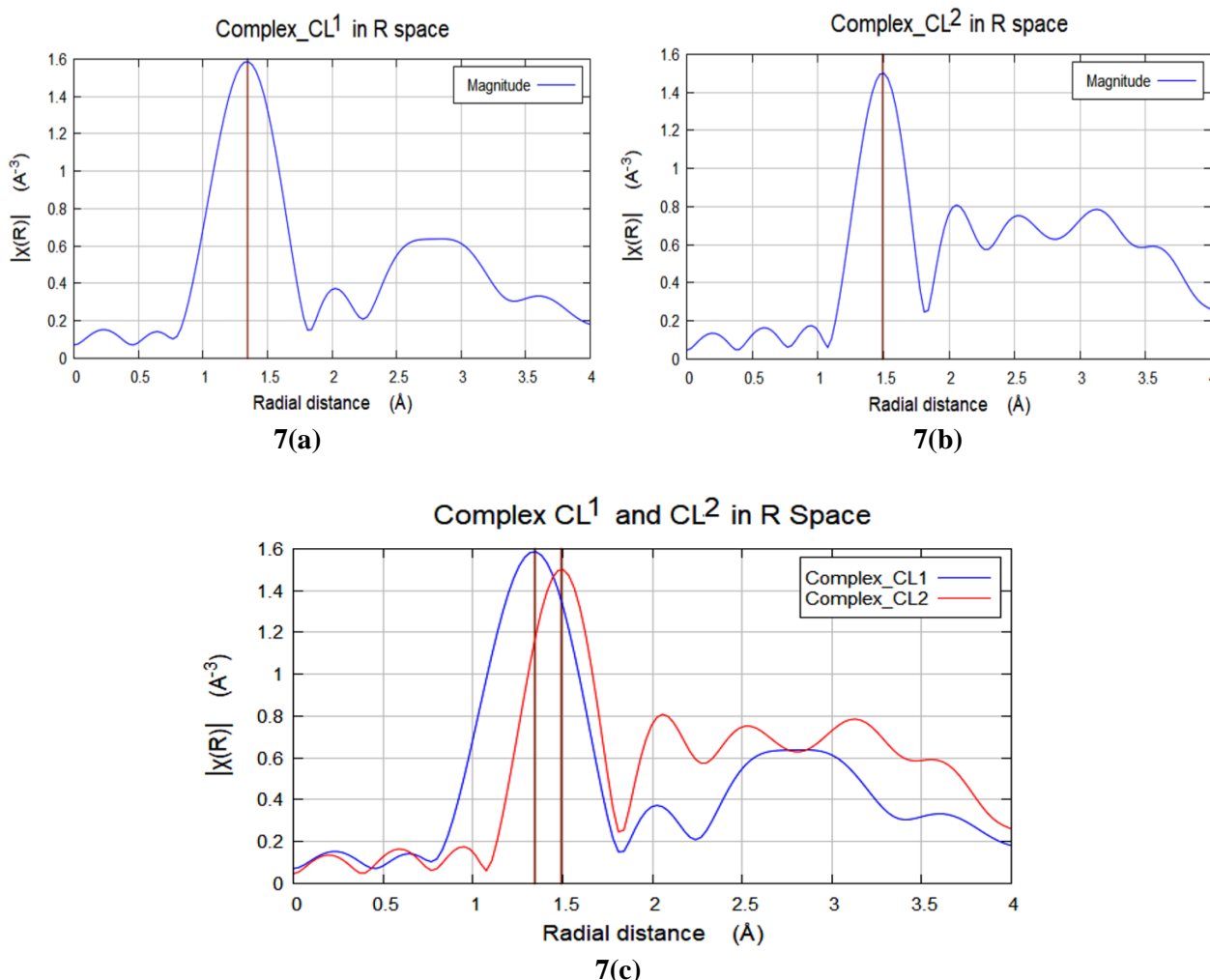


**Figure 7(a,b and c).** Magnitude of Fourier Transform of Complex CL<sup>1</sup>, Complex CL<sup>2</sup> and Fourier transforms of Combined Complex CL<sup>1</sup>, Complex CL<sup>2</sup>

**Table 4.** Bond length values obtained for the complexes CL<sup>1</sup> and CL<sup>2</sup>.

S.No.	Name of Complex	Phase Corrected		Phase uncorrected	
		Levy's method Å	Lytle method Å	L.S.S. Method R1- α1 Å	F.T. method R Å
2.	Complex CL <sup>1</sup>	1.74	1.92	1.21	1.35
3.	Complex CL <sup>2</sup>	1.72	1.90	1.38	1.49

#### 4. Conclusion

In the current work, calculations of copper metal and its complexes CL<sup>1</sup> and CL<sup>2</sup> were performed using XRD, FTIR, XANES and EXAFS data [32].

FTIR patterns were used to confirm the presence of functional groups and structural parameters in the investigated complexes. The X-ray diffraction patterns were examined to determine the crystal

structure, space group, particle size, etc. The chemical shifts, PAM shifts and edge widths of the complexes were calculated to be 6.55eV, 5.35eV and 12.39 eV for complex CL<sup>1</sup> and 3.75eV, -8.9eV and 11.64eV for complex CL<sup>2</sup>, respectively. Compared to copper metal, PAM is shifted to lower energies. Moreover, PAM from complex CL<sup>2</sup> shows a higher shift than complex CL<sup>1</sup>. The PAM shift of the complex is opposite to the chemical shift. These reversible orders demonstrate that PAM changes are inversely proportional to complex ionicity [31–32]. The effective nuclear charge (ENC) values for complexes CL<sup>1</sup> and CL<sup>2</sup> are 0.45 and 0.26 electrons/atom, respectively. According to chemical shift values, copper is present in both complexes in the +2 oxidation state [33]. Three graphics approaches: Levy's, Lytle's and L.S.S. approach was used to determine the bond length of the complex from the maximum and minimum values of EXAFS. Bond lengths were determined using Athena software. The bond lengths calculated using the Lytle, Sayers, and Stern (L.S.S.) method and the results of the Fourier transform method are in strong agreement. Applications in the biological, chemical, and pharmaceutical industries in general can benefit from the results of the studied conjugates.

## 5. References

- Shalin Kumar, DurgaNath Dhar and P N Saxena, Jour. Of Scientific & Industrial Res, Vol 68(March 2009) 181-187
- Mayank Sharma, J. Tripathi, A. Mishra, A.K. Yadav, S.N Jha, B. D. Shrivastava, Materials Today: Proceedings 12(2019) 614-620
- A. Sethukumar, B. Arul Prakasam Journal of Molecular Structure 963 (2010) 250–257
- H.G. Grag, C. Prakash, J. Pharm. Sci. 60 (1971) 323.
- M.K. Jani, N.K. Undavia, P.B. Trivedi, J. Indian Chem. Soc. 67 (7) (1990) 601.
- S. GunizKucukguzel, Eur. J. Med. Chem. 34 (1999) 1093.
- Kritika Shukla, PradeepSharma, Ashutosh Mishra, Russ. J. Physical Chemistry Chem. **95**, S128–S139 (2021).
- A. P. Mishra and M. Soni, Met.-Based Drugs 2008, 1 (2008).
- Y. Song, Z. Xu, Q. Sun, B. Su, Q. Gao, H. Liu, and J. Zhao, J. Coord. Chem. 61, 1212 (2008).
- N. Raman, S. J. Raja, and A. Sakthivel, J. Coord. Chem. 62, 691 (2009).
- G. Grivani, V. Tahmasebi, A. D. Khalaji, K. Fejfarovac, and M. Dusek, Polyhedron 51, 54 (2013).
- Kamran T. Mahmudov, Maximilian N. Kopylovich, M. Fátima C. Guedes da Silva, Gunay S. Mahmudova, Manas Sutradhar, Armando J.L. Pombeiro, Polyhedron 60 (2013)78-84.
- A F Shoair, A A El-Bindary, El-Ghamaz, G.N. Rezk “Synthesis, characterization, DNA binding and antitumor activities of Cu(II) complexes”, Journal of molecular liquid, 2018.08.075.
- H. C. Yao and J. Org. Chem. 29, 2959-2963 (1964).
- K. T. Mahamudov, M. N. Kopylovich, M. F. Da silva, G. S. Mahamudova, M. Sutradhar and A. J. L. Pombeiro, Polyhedron 60, 78-84 (2013).
- M. N. Kopylovich, K. T. Mahamudov, M. Haukka, K. V. Luzyanin and A. G. L. Pombeiro, Inorg. Chem. Acta 374, 175-180 (2011).
- A.Y. Lee, D.Y. Park, and M. S. Jeong, J. Alloys Compd., vol. 738, pp. 239-245, Mar.2018
- A. Gaur, A. Johri, B. D. Shrivastava, D. Gaur, S. N. Jha, D. Bhattacharya, A. Poswal and S. K. Deb, Sadhana 36, 339-348 (2011)
- M. Bouhdada, M. E. L. Amane, B. B. Mohammed, and K. Yamni, J. Mol. Struct. 1177, 391 (2019).
- M. Sharma, J. Tripathi, A. Mishra, A. K. Yadav, S. N. Jha, and B. D. Shrivastava, Mater. Today: Proc. 12, 614 (2019).
- A. Drzewiecka, A. E. Koziol, M. T. Klepka, A. Wolska, S. B. Jimenez-Pulido, T. Lis, K. Ostrowska, and M. Struga, Chem. Phys. Lett. 559, 41 (2013).
- A. Gaur, N. N. Nair, B. D. Shrivastava, B. K. Das, M. Chakraborty, and S. N. Jha, Chem. Phys. Lett. 692, 382 (2018).
- S. B. Erenburg, S. V. Trubina, and N. N. Golovnev, Russ. J. Phys. Chem. 87, 461 (2013).
- B. R. Tagirov, A. L. Trigub, P. V. Selivanov, and L. A. Koroleva, Russ. J. Phys. Chem. A 91, 543 (2017).
- O. P. Tkachenko and L. M. Kustov, Russ. J. Phys. Chem. A 87, 935 (2013). 28. A. S. Burlova, A. I. Uraev, D. A. Garnovskii, K. A. Ly
- A. S. Burlova, A. I. Uraev, D. A. Garnovskii, K. A. Lyssenko, V. G. Vlasenko, Y. V. Zubavichus, V. Yu. Murzin, E. V. Korshunova, G. S. Borodkin, S. I.



- Levchenkov, I. S. Vasilchenko, and V. I. Minkin, *J. Mol. Struct.* 1064, 111 (2014).
27. Parsai Neetu, Mishra Ashutosh, and Shrivastava B D, 2013 *Indian journal of pure and applied physics* **51** 185-190
  28. Gianturco F A and Coulson C A 1968 *Molec. Phys.* **14** 223
  29. Gaur Abhijeet, Shrivastava B D, and Nigam H L 2013 *Proc. Indian Natn. Sci. Acad.* **79** 921- 966
  30. Leavy R M 1965j. *Chemis. Phys.* 431846
  31. Nair Nitin N et al. 2016 *J. Physics: Conference series*, **755** 012012
  32. <http://www.rrcat.gov.in/technology/accel/srul/beamlines/exafsscan.html>
  33. Sharma Mayank, Tripathi J, Mishra A, Yadav A K, Jha S N and Shrivastava B D 2019 *Materials Today: Proceedings* **12** 614-620